

A 3D breakable Grain-Based Discrete Element model for transversely isotropic rocks

Leandro Lima Rasmussen

Department of Civil and Environmental Engineering, University of Brasilia, Brazil

Department of Energy Systems Engineering and Research Institute of Energy and Resources, Seoul National University, Republic of Korea

Ki-Bok Min

Department of Energy Systems Engineering and Research Institute of Energy and Resources, Seoul National University, Republic of Korea

ABSTRACT: This research proposes a novel Grain-Based Model (GBM) for the simulation of transversely isotropic rocks. The model introduces Rigid Body Spring Network bonds and a fictitious stress approach into the Discrete Element Method in order to generate the anisotropic elastic behavior and utilizes breakable particles to manifest cleavage failure. The new model is verified by comparing numerical stress bulbs from a point load analysis against a finite element solution and by comparing unconfined compression strength test results from Asan Gneiss GBM against Jaeger's 'plane of weakness' theory. Of note, the novel grain-based model allowed the direct determination of macroscale anisotropy in elastic and strength properties without the need for trial-and-error calibrations of input parameters. In addition, the proposed breakable grain scheme provided for realistic representations of the failure modes usually observed in rocks with cleavage.

Keywords: Hybrid LDEM, RBSN-DEM, Transversely isotropic rock, Breakable particle.

1 INTRODUCTION

The majority of numerical research that applied the Discrete Element Method to the analysis of transversely isotropic rocks used the Bonded Particle Model (BPM) technique (Potyondy & Cundall 2004), with Smooth Joints (Ivars et al. 2008) generating the numerical representation of cleavage planes and anisotropy in deformability and strength (e.g., Park & Min 2015 and Zhao et al. 2022). Alternatively, the Grain-Based Model (GBM) or Bonded Block Model (BBM) technique has also been used (Lan et al. 2010), with tetrahedral particles replacing spherical ones. In GBM, anisotropy was introduced by means of particles elongated in the direction of isotropy plane (Ghazvinian et al. 2014) or using geometry that conformed to the cleavage planes orientation (Huang et al. 2022).

Both BPM and GBM/BBM techniques have attracted the attention of researchers in rock mechanics due to their ability in investigating realistic failure phenomena while grounded on simple theories and assumptions. On the other hand, trial-and-error calibration is necessary to define the model's input parameters that can provide a match with properties observed in laboratory.

The objective of this study is to propose and investigate two contributions to enhance the GBM/BBM technique for the simulation of transversely isotropic rocks: the adoption of Rigid Body

Spring Network bonds combined with a fictitious stress method for generating the anisotropy in elastic behavior; and a novel breakable grain scheme for the manifestation of cleavage fracture without the need for preconditioned meshes or Smooth Joints.

2 THEORY

2.1 The Hybrid Lattice/Discrete Element Method

The Hybrid Lattice/Discrete Element Method (Rasmussen 2021) consists in the combination of Rigid Body Spring Network (RBSN) Lattice bonds (Bolander & Saito 1998) with the Discrete Element Method (Hart et al. 1988) using Voronoi cells. Figure 1 shows the RBSN bond, consisting of a set of three linear and rotational springs positioned at the centroid of each facet between Voronoi cells.

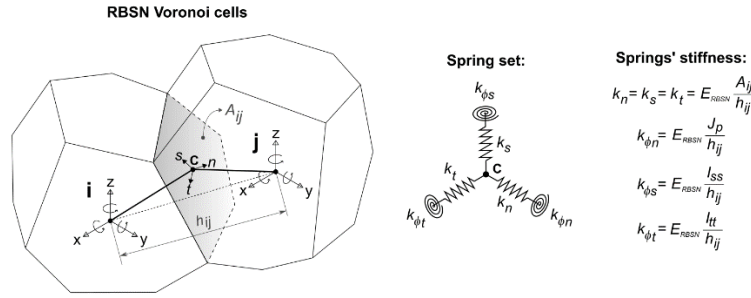


Figure 1. RBSN bond between Voronoi cells and set of springs with their stiffness values calculated based on the facet's area, principal moments of inertia, Young's modulus and the distance between cells' nuclei.

The Hybrid scheme combines advantageous characteristics of both RBSN and DEM: while RBSN bonds are capable of generating elastically homogeneous material behavior with mesh objectivity, DEM allows large displacements and rotations to occur, with contact detection mechanism operating.

For generating the elastic behavior of transversely isotropic materials in RBSN, a fictitious stress method was proposed (Rasmussen & Assis 2018). At each time-step of the simulation, a fictitious stress tensor is calculated according to the five independent elastic parameters to generate fictitious forces into the RBSN bonds, as shown in Figure 2.

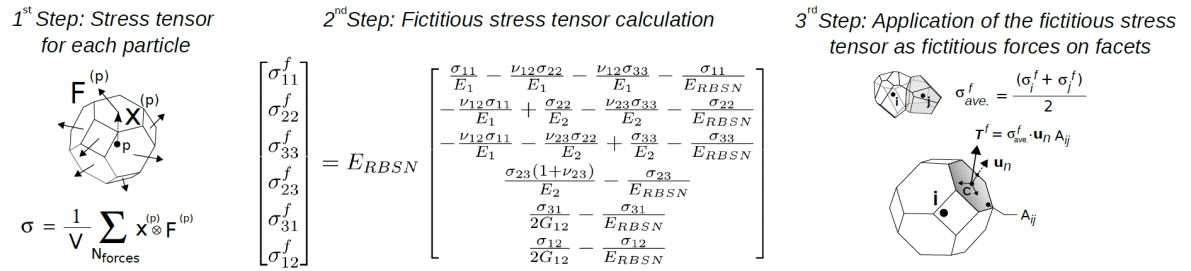


Figure 2. The fictitious stress method for the realization of transversely isotropic elastic behavior in RBSN (Rasmussen & Assis 2018). Index 1 refers to the direction perpendicular to the isotropy plane orientation.

In this work, the fictitious stress method has been incorporated into the Hybrid Lattice/Discrete Element Method framework for simulating the elastic behavior of transversely isotropic rocks.

For rupture, during a simulation, mode-I fracture of the RBSN bonds is verified by comparing an estimate of the maximum tensile stress (σ_{max}^b) against the bond's tensile strength (σ_t^b):

$$\sigma_{max}^b = \frac{F_n}{A_{ij}} + \frac{\sqrt{M_s^2 + M_t^2}}{I_{disk}} R_{disk} \geq \sigma_t^b \quad (1)$$

where I_{disk} and R_{disk} are the moment of inertia and radius of a disk with area equal to that of the bonded facet A_{ij} . At the same time, mode-II fracture takes place if the maximum shear stress (τ_{max}^b) is higher than the shear strength, defined by the bond cohesion intercept (c^b) and friction angle (ϕ^b):

$$\tau_{max}^b = \frac{\sqrt{F_s^2 + F_t^2}}{A_{ij}} + \frac{|M_n|R_{disk}}{J_{disk}} \geq c^b + \frac{\langle -F_n \rangle}{A_{ij}} \tan(\phi^b) \quad (2)$$

2.2 A replaceable particle scheme for cleavage fracture

A novel replaceable particle scheme is proposed for manifesting cleavage fracture in GBM. In this scheme, the stress tensor for each particle is calculated by means of homogenization theory and used to estimate the normal and shear stress on the cleavage plane that cross the particle. During simulation, the particle separates along the cleavage plane when a Mohr-Coulomb strength criterion with tension cut-off is met, as illustrated in Figure 3.

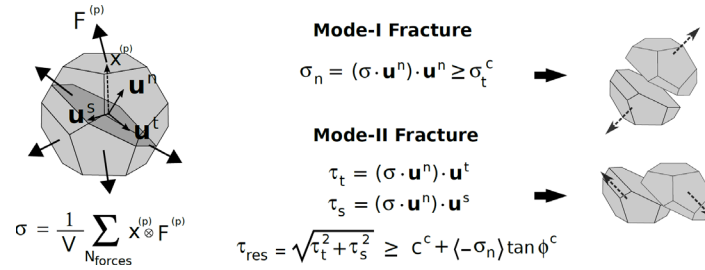


Figure 3. The proposed replaceable particle scheme for the simulation of cleavage fracture. σ_t^c , c^c and ϕ^c are the cleavage's tensile strength, cohesion intercept and friction angle respectively.

3 VERIFICATION

3.1 Point load on a transversely isotropic continuum medium

The comparison between the bulb stresses due to a vertical concentrated load on a continuum transversely isotropic medium from a Hybrid LDEM GBM and a FEM simulation served to further verify the accuracy of the elastic behavior of the proposed model.

The simulations employed the following elastic parameters: $E_1 = 30$ GPa, $E_2 = 70$ GPa, $G_{12} = 20$ GPa, $\nu_{12} = 0.2$, and $\nu_{23} = 0.3$. E_{RBSN} does not impact the results and was set equal to E_1 . Three different loading orientation angles were investigated: vertical ($\theta = 0^\circ$), inclined ($\theta = 60^\circ$), and horizontal ($\theta = 90^\circ$) isotropy plane orientations. Figure 4 shows the model dimensions, boundary conditions and mesh adopted for both the GBM and FEM models.

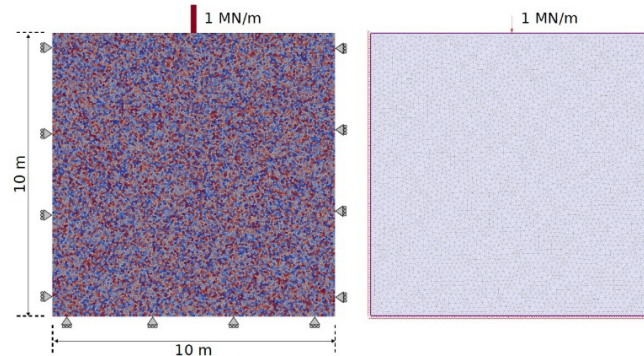


Figure 4. Grain-based (left) and Finite Element (right) models for the point load analysis.

Figure 5 presents the bulb stresses, defined by the minimum principal stress σ_3 (compression), calculated from both models. The figure indicates that the minimum principal stress distributions from the Hybrid LDEM GBM and FEM models presented an almost indistinguishable resemblance.

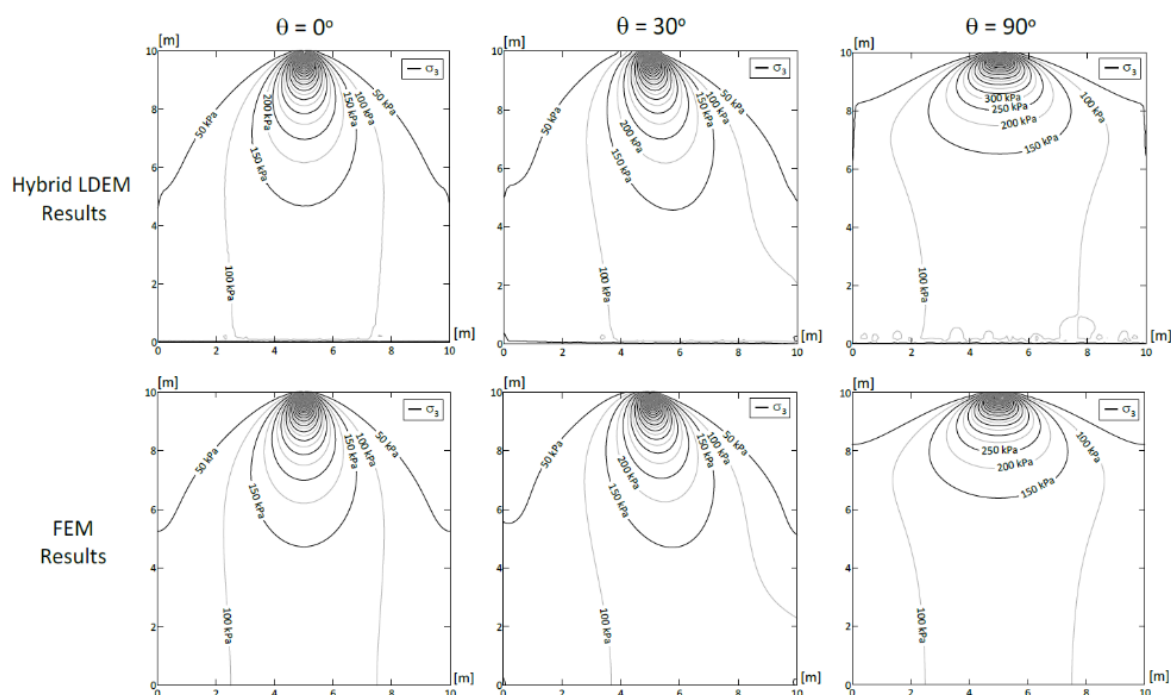


Figure 5. Minimum principal stress distributions from the Hybrid LDEM GBM and FEM models.

3.2 Elastic and strength anisotropy of Asan Gneiss

Uniaxial compression and Brazilian tensile tests were conducted for characterizing the anisotropy in strength of deformability behavior of Asan gneiss (Cho et al. 2012). From these results, the strength parameters were calculated according to Jaeger's 'plane of weakness' theory (Jaeger 1960). Table 1 shows the deformability and strength parameters for Asan Gneiss estimated from the laboratory tests.

Table 1. Deformability and strength parameters for Asan Gneiss estimated from the laboratory tests.

Parameter		Value
<i>Elastic parameters</i>	Elastic modulus E_1 [GPa]	54.4
	Elastic modulus E_2 [GPa]	68.3
	Poisson's ratio ν_{12}	0.2
	Poisson's ratio ν_{23}	0.3
	Shear modulus G_{12} [GPa]	17.1
<i>Bond strength parameters</i>	Tensile strength σ_t^b [MPa]	14.5
	Cohesion c^b [MPa]	59.8
	Friction angle ϕ^b [$^\circ$]	21.9
<i>Cleavage strength parameters</i>	Tensile strength σ_t^c [MPa]	6.9
	Cohesion c^c [MPa]	57.6
	Friction angle ϕ^c [$^\circ$]	0

A Hybrid LDEM GBM was developed for Asan Gneiss, with the laboratory estimated properties shown in Table 1 being directly introduced as numerical input parameters, without trial-and-error calibration. For the GBM, a cylindrical shape was selected, with a diameter of 54 mm and a height of 135 mm, and a fine mesh discretization was adopted, with approximately 1,000 Voronoi cells.

Unconfined compression tests were conducted numerically. For the loading, plates were attached to the top and bottom parts of the model and were assigned a constant velocity of 4 cm/s. Particles density was set equal to 2,500 kg/m³ and a non-viscous local damping factor of 0.3 was adopted. The residual friction angle and contact stiffness between unbonded particles was set equal to 18° and 1,5 GN/m respectively.

Figure 6 shows the apparent variation in Young's modulus and unconfined compression strength for different loading orientation angles. This figure also presents the theoretical curves according to continuum mechanics theory for transversely isotropic elastic materials and Jaeger's 'plane of weakness' theory (Jaeger 1960). It is observed that the variation in numerical results with loading orientation angle plotted practically on top of the theoretical curves.

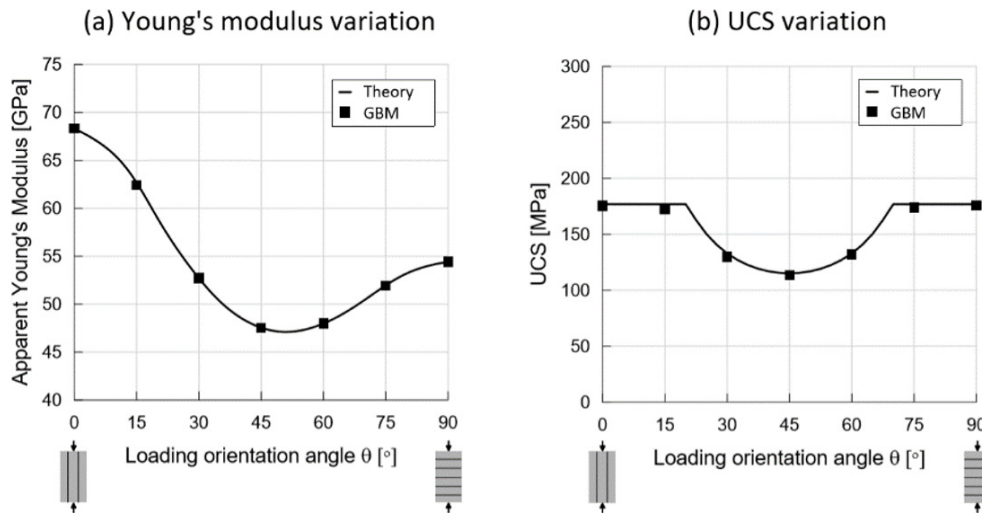


Figure 6. Variation in (a) apparent Young's modulus and (b) unconfined compression strength for Asan gneiss GBM and curves showing the theoretical variations.

A side-by-side comparison between the failure modes observed in the numerical and laboratory unconfined compression tests is presented in Figure 7. This figure indicates that the Asan Gneiss GBM presented realistic failure modes, compatible with those reported in literature for transversely isotropic rocks with cleavage planes.

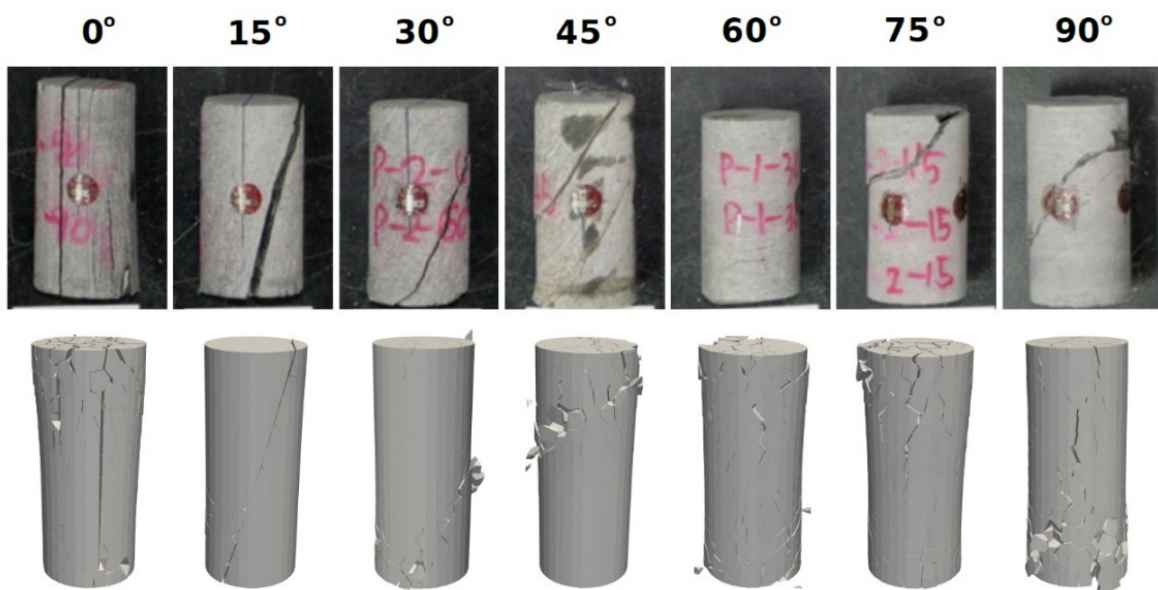


Figure 7. Laboratory and numerically observed failure modes for Asan gneiss GBM from the UCS tests.

4 CONCLUSION

A novel three-dimensional Grain-Based Model for the Discrete Element Method has been developed and investigated for the simulation of transversely isotropic rocks. The use of Rigid Body Spring Network bonds of Bolander & Saito (1998) along with the fictitious stress method of Rasmussen & Assis (2018) in DEM generated GBMs with transversely isotropic elastic behavior with due consideration of all five independent elastic parameters. Of note, the new GBM did not require trial-and-error calibration of its numerical input parameters in order to represent the anisotropy in deformability and peak strength behavior. The proposed replaceable particle scheme allowed the manifestation of cleavage fracture and realistic failure modes in unconfined compression tests without the need for preconditioned meshes or the use of Smooth Joints.

ACKNOWLEDGEMENTS

This work has been supported by the Basic Science Research Program through the National Research Foundation of Korea (NRF) funded by the Korea government (MSIT) (grant 2021M2E3A2044264) and by the Seoul National University Energy Resources Engineering Global Scholarship.

REFERENCES

- Bolander, J. & Saito, S. 1998. Fracture analyses using spring networks with random geometry. *Engineering Fracture Mechanics*;61(5):569 _ 591. DOI:[https://doi.org/10.1016/S0013-7944\(98\)00069-1](https://doi.org/10.1016/S0013-7944(98)00069-1)
- Cho, J.W., Kim, H., Jeon, S. & Min, K.B. 2012. Deformation and strength anisotropy of asan gneiss, boryeong shale, and yeoncheon schist. *International Journal of Rock Mechanics and Mining Sciences* 50, pp. 158-169. DOI:<https://doi.org/10.1016/j.ijrmms.2011.12.004>
- Ghazvinian, E., Diederichs, M. & Quey, R. 2014. 3d random voronoi grain-based models for simulation of brittle rock damage and fabric-guided micro-fracturing. *Journal of Rock Mechanics and Geotechnical Engineering* 6 (6), pp. 506-521. DOI:<https://doi.org/10.1016/j.jrmge.2014.09.001>
- Hart, R., Cundall, P. & Lemos, J. 1988. Formulation of a three-dimensional distinct element model part II. mechanical calculations for motion and interaction of a system composed of many polyhedral blocks. *International Journal of Rock Mechanics and Mining Sciences & Geomechanics Abstracts* 25 (3), pp. 117-125. DOI:[https://doi.org/10.1016/0148-9062\(88\)92294-2](https://doi.org/10.1016/0148-9062(88)92294-2)
- Huang, J., Song, Y., Lei, M., Shi, C., Jia, C. & Zhang, J. 2022. Numerical simulation of anisotropic properties of shale under triaxial compression using 3d dem. *Research Square*. DOI:10.21203/rs.3.rs-2024410/v1.
- Ivars, D.M., Potyondy, D.O., Pierce, M.E. & Cundall, P.A. 2008. The smooth-joint contact model. In: 8th. *World Congress on Computational Mechanics*. Venice, Italy.
- Jaeger, J.C. 1960. Shear failure of anisotropic rocks. *Geological Magazine* 97 (1), pp. 65-72. DOI:10.1017/S0016756800061100
- Lan, H., Martin, C.D. & Hu, B. 2010. Effect of heterogeneity of brittle rock on micromechanical extensile behavior during compression loading. *Journal of Geophysical Research: Solid Earth* 115 (B1). DOI:10.1029/2009JB006496
- Park, B. & Min, K.B. 2015. Bonded-particle discrete element modeling of mechanical behavior of transversely isotropic rock. *International Journal of Rock Mechanics and Mining Sciences* 76, pp. 243-255. DOI:<https://doi.org/10.1016/j.ijrmms.2015.03.014>
- Potyondy, D. & Cundall, P.A. 2004. A Bonded-particle model for rock. *International Journal of Rock Mechanics and Mining Sciences* 41(8), pp. 1329-1364. DOI:<https://doi.org/10.1016/j.ijrmms.2004.09.011>
- Rasmussen, L.L. & Assis, A.P. 2018. Elastically-homogeneous lattice modelling of transversely isotropic rocks. *Computers and Geotechnics* 104, pp. 96-108. DOI:<https://doi.org/10.1016/j.compgeo.2018.08.016>
- Rasmussen, L.L. 2021. Hybrid lattice/discrete element method for bonded block modeling of rocks. *Computers and Geotechnics* 130, pp. 103907. DOI:<https://doi.org/10.1016/j.compgeo.2020.103907>
- Zhao, Y., Mishra, B., Shi, Q. & Zhao, G. 2022. A size-dependent bonded-particle model for transversely isotropic rock and its application in studying the size effect of shale. *Geotech Geol Eng* 40, pp. 5437-5453. DOI:<https://doi.org/10.1007/s10706-022-02224-4>